

Measurement of the B^+/B^0 Production Ratio from the $\Upsilon(4S)$ Meson using
 $B^+ \rightarrow J/\psi K^+$ and $B^0 \rightarrow J/\psi K_s^0$ Decays

B. Aubert,¹ R. Barate,¹ D. Boutigny,¹ F. Couderc,¹ J.-M. Gaillard,¹ A. Hicheur,¹ Y. Karyotakis,¹ J. P. Lees,¹
V. Tisserand,¹ A. Zghiche,¹ A. Palano,² A. Pompili,² J. C. Chen,³ N. D. Qi,³ G. Rong,³ P. Wang,³ Y. S. Zhu,³
G. Eigen,⁴ I. Ofte,⁴ B. Stugu,⁴ G. S. Abrams,⁵ A. W. Borgland,⁵ A. B. Breon,⁵ D. N. Brown,⁵ J. Button-Shafer,⁵
R. N. Cahn,⁵ E. Charles,⁵ C. T. Day,⁵ M. S. Gill,⁵ A. V. Gritsan,⁵ Y. Groysman,⁵ R. G. Jacobsen,⁵
R. W. Kadel,⁵ J. Kadyk,⁵ L. T. Kerth,⁵ Yu. G. Kolomensky,⁵ G. Kukartsev,⁵ C. LeClerc,⁵ M. E. Levi,⁵
G. Lynch,⁵ L. M. Mir,⁵ P. J. Oddone,⁵ T. J. Orimoto,⁵ M. Pripstein,⁵ N. A. Roe,⁵ M. T. Ronan,⁵ V. G. Shelkov,⁵
A. V. Telnov,⁵ W. A. Wenzel,⁵ K. Ford,⁶ T. J. Harrison,⁶ C. M. Hawkes,⁶ S. E. Morgan,⁶ A. T. Watson,⁶
N. K. Watson,⁶ M. Fritsch,⁷ K. Goetzen,⁷ T. Held,⁷ H. Koch,⁷ B. Lewandowski,⁷ M. Pelizaeus,⁷ M. Steinke,⁷
J. T. Boyd,⁸ N. Chevalier,⁸ W. N. Cottingham,⁸ M. P. Kelly,⁸ T. E. Latham,⁸ F. F. Wilson,⁸ K. Abe,⁹
T. Cuhadar-Donszelmann,⁹ C. Hearty,⁹ T. S. Mattison,⁹ J. A. McKenna,⁹ D. Thiessen,⁹ P. Kyberd,¹⁰
L. Teodorescu,¹⁰ V. E. Blinov,¹¹ A. D. Bukin,¹¹ V. P. Druzhinin,¹¹ V. B. Golubev,¹¹ V. N. Ivanchenko,¹¹
E. A. Kravchenko,¹¹ A. P. Onuchin,¹¹ S. I. Serednyakov,¹¹ Yu. I. Skovpen,¹¹ E. P. Solodov,¹¹ A. N. Yushkov,¹¹
D. Best,¹² M. Bruinsma,¹² M. Chao,¹² I. Eschrich,¹² D. Kirkby,¹² A. J. Lankford,¹² M. Mandelkern,¹²
R. K. Mommsen,¹² W. Roethel,¹² D. P. Stoker,¹² C. Buchanan,¹³ B. L. Hartfiel,¹³ J. W. Gary,¹⁴ B. C. Shen,¹⁴
K. Wang,¹⁴ D. del Re,¹⁵ H. K. Hadavand,¹⁵ E. J. Hill,¹⁵ D. B. MacFarlane,¹⁵ H. P. Paar,¹⁵ Sh. Rahatlou,¹⁵
V. Sharma,¹⁵ J. W. Berryhill,¹⁶ C. Campagnari,¹⁶ B. Dahmes,¹⁶ S. L. Levy,¹⁶ O. Long,¹⁶ A. Lu,¹⁶ M. A. Mazur,¹⁶
J. D. Richman,¹⁶ W. Verkerke,¹⁶ T. W. Beck,¹⁷ A. M. Eisner,¹⁷ C. A. Heusch,¹⁷ W. S. Lockman,¹⁷ T. Schalk,¹⁷
R. E. Schmitz,¹⁷ B. A. Schumm,¹⁷ A. Seiden,¹⁷ P. Spradlin,¹⁷ D. C. Williams,¹⁷ M. G. Wilson,¹⁷ J. Albert,¹⁸
E. Chen,¹⁸ G. P. Dubois-Felsmann,¹⁸ A. Dvoretzskii,¹⁸ D. G. Hitlin,¹⁸ I. Narsky,¹⁸ T. Piatenko,¹⁸ F. C. Porter,¹⁸
A. Ryd,¹⁸ A. Samuel,¹⁸ S. Yang,¹⁸ S. Jayatilleke,¹⁹ G. Mancinelli,¹⁹ B. T. Meadows,¹⁹ M. D. Sokoloff,¹⁹
T. Abe,²⁰ F. Blanc,²⁰ P. Bloom,²⁰ S. Chen,²⁰ P. J. Clark,²⁰ W. T. Ford,²⁰ U. Nauenberg,²⁰ A. Olivas,²⁰
P. Rankin,²⁰ J. G. Smith,²⁰ W. C. van Hoek,²⁰ L. Zhang,²⁰ J. L. Harton,²¹ T. Hu,²¹ A. Soffer,²¹ W. H. Toki,²¹
R. J. Wilson,²¹ D. Altenburg,²² T. Brandt,²² J. Brose,²² T. Colberg,²² M. Dickopp,²² E. Feltresi,²² A. Hauke,²²
H. M. Lacker,²² E. Maly,²² R. Müller-Pfefferkorn,²² R. Nogowski,²² S. Otto,²² J. Schubert,²² K. R. Schubert,²²
R. Schwierz,²² B. Spaan,²² D. Bernard,²³ G. R. Bonneaud,²³ F. Brochard,²³ P. Grenier,²³ Ch. Thiebaut,²³
G. Vasileiadis,²³ M. Verderi,²³ D. J. Bard,²⁴ A. Khan,²⁴ D. Lavin,²⁴ F. Muheim,²⁴ S. Playfer,²⁴ M. Andreotti,²⁵
V. Azzolini,²⁵ D. Bettoni,²⁵ C. Bozzi,²⁵ R. Calabrese,²⁵ G. Cibinetto,²⁵ E. Luppi,²⁵ M. Negrini,²⁵ A. Sarti,²⁵
E. Treadwell,²⁶ R. Baldini-Ferroli,²⁷ A. Calcaterra,²⁷ R. de Sangro,²⁷ G. Finocchiaro,²⁷ P. Patteri,²⁷ M. Piccolo,²⁷
A. Zallo,²⁷ A. Buzzo,²⁸ R. Capra,²⁸ R. Contri,²⁸ G. Crosetti,²⁸ M. Lo Vetere,²⁸ M. Macri,²⁸ M. R. Monge,²⁸
S. Passaggio,²⁸ C. Patrignani,²⁸ E. Robutti,²⁸ A. Santroni,²⁸ S. Tosi,²⁸ S. Bailey,²⁹ G. Brandenburg,²⁹ M. Morii,²⁹
E. Won,²⁹ R. S. Dubitzky,³⁰ U. Langenegger,³⁰ W. Bhimji,³¹ D. A. Bowerman,³¹ P. D. Dauncey,³¹ U. Egede,³¹
J. R. Gaillard,³¹ G. W. Morton,³¹ J. A. Nash,³¹ G. P. Taylor,³¹ G. J. Grenier,³² S.-J. Lee,³² U. Mallik,³²
J. Cochran,³³ H. B. Crawley,³³ J. Lamsa,³³ W. T. Meyer,³³ S. Prell,³³ E. I. Rosenberg,³³ J. Yi,³³ M. Davier,³⁴
G. Grosdidier,³⁴ A. Höcker,³⁴ S. Laplace,³⁴ F. Le Diberder,³⁴ V. Lepeltier,³⁴ A. M. Lutz,³⁴ T. C. Petersen,³⁴
S. Plaszczynski,³⁴ M. H. Schune,³⁴ L. Tantot,³⁴ G. Wormser,³⁴ C. H. Cheng,³⁵ D. J. Lange,³⁵ M. C. Simani,³⁵
D. M. Wright,³⁵ A. J. Bevan,³⁶ J. P. Coleman,³⁶ J. R. Fry,³⁶ E. Gabathuler,³⁶ R. Gamet,³⁶ M. Kay,³⁶ R. J. Parry,³⁶
D. J. Payne,³⁶ R. J. Sloane,³⁶ C. Touramanis,³⁶ J. J. Back,³⁷ P. F. Harrison,³⁷ G. B. Mohanty,³⁷ C. L. Brown,³⁸
G. Cowan,³⁸ R. L. Flack,³⁸ H. U. Flaecher,³⁸ S. George,³⁸ M. G. Green,³⁸ A. Kurup,³⁸ C. E. Marker,³⁸
T. R. McMahon,³⁸ S. Ricciardi,³⁸ F. Salvatore,³⁸ G. Vaitsas,³⁸ M. A. Winter,³⁸ D. Brown,³⁹ C. L. Davis,³⁹
J. Allison,⁴⁰ N. R. Barlow,⁴⁰ R. J. Barlow,⁴⁰ P. A. Hart,⁴⁰ M. C. Hodgkinson,⁴⁰ G. D. Lafferty,⁴⁰ A. J. Lyon,⁴⁰
J. C. Williams,⁴⁰ A. Farbin,⁴¹ W. D. Hulsbergen,⁴¹ A. Jawahery,⁴¹ D. Kovalskyi,⁴¹ C. K. Lae,⁴¹ V. Lillard,⁴¹
D. A. Roberts,⁴¹ G. Blaylock,⁴² C. Dallapiccola,⁴² K. T. Flood,⁴² S. S. Hertzbach,⁴² R. Kofler,⁴² V. B. Koptchev,⁴²
T. B. Moore,⁴² S. Saremi,⁴² H. Staengle,⁴² S. Willocq,⁴² R. Cowan,⁴³ G. Sciolla,⁴³ F. Taylor,⁴³ R. K. Yamamoto,⁴³
D. J. J. Mangeol,⁴⁴ P. M. Patel,⁴⁴ S. H. Robertson,⁴⁴ A. Lazzaro,⁴⁵ F. Palombo,⁴⁵ J. M. Bauer,⁴⁶ L. Cremaldi,⁴⁶
V. Eschenburg,⁴⁶ R. Godang,⁴⁶ R. Kroeger,⁴⁶ J. Reidy,⁴⁶ D. A. Sanders,⁴⁶ D. J. Summers,⁴⁶ H. W. Zhao,⁴⁶
S. Brunet,⁴⁷ D. Côté,⁴⁷ P. Taras,⁴⁷ H. Nicholson,⁴⁸ C. Cartaro,⁴⁹ N. Cavallo,⁴⁹ F. Fabozzi,⁴⁹ * C. Gatto,⁴⁹
L. Lista,⁴⁹ D. Monorchio,⁴⁹ P. Paolucci,⁴⁹ D. Piccolo,⁴⁹ C. Sciacca,⁴⁹ M. Baak,⁵⁰ G. Raven,⁵⁰ L. Wilden,⁵⁰
C. P. Jessop,⁵¹ J. M. LoSecco,⁵¹ T. A. Gabriel,⁵² T. Allmendinger,⁵³ B. Brau,⁵³ K. K. Gan,⁵³ K. Honscheid,⁵³

D. Hufnagel,⁵³ H. Kagan,⁵³ R. Kass,⁵³ T. Pulliam,⁵³ R. Ter-Antonyan,⁵³ Q. K. Wong,⁵³ J. Brau,⁵⁴ R. Frey,⁵⁴ O. Igonkina,⁵⁴ C. T. Potter,⁵⁴ N. B. Sinev,⁵⁴ D. Strom,⁵⁴ E. Torrence,⁵⁴ F. Colecchia,⁵⁵ A. Dorigo,⁵⁵ F. Galeazzi,⁵⁵ M. Margoni,⁵⁵ M. Morandin,⁵⁵ M. Posocco,⁵⁵ M. Rotondo,⁵⁵ F. Simonetto,⁵⁵ R. Stroili,⁵⁵ G. Tiozzo,⁵⁵ C. Voci,⁵⁵ M. Benayoun,⁵⁶ H. Briand,⁵⁶ J. Chauveau,⁵⁶ P. David,⁵⁶ Ch. de la Vaissière,⁵⁶ L. Del Buono,⁵⁶ O. Hamon,⁵⁶ M. J. J. John,⁵⁶ Ph. Leruste,⁵⁶ J. Ocariz,⁵⁶ M. Pivk,⁵⁶ L. Roos,⁵⁶ S. T'Jampens,⁵⁶ G. Therin,⁵⁶ P. F. Manfredi,⁵⁷ V. Re,⁵⁷ P. K. Behera,⁵⁸ L. Gladney,⁵⁸ Q. H. Guo,⁵⁸ J. Panetta,⁵⁸ F. Anulli,^{27,59} M. Biasini,⁵⁹ I. M. Peruzzi,^{27,59} M. Pioppi,⁵⁹ C. Angelini,⁶⁰ G. Batignani,⁶⁰ S. Bettarini,⁶⁰ M. Bondioli,⁶⁰ F. Bucci,⁶⁰ G. Calderini,⁶⁰ M. Carpinelli,⁶⁰ V. Del Gamba,⁶⁰ F. Forti,⁶⁰ M. A. Giorgi,⁶⁰ A. Lusiani,⁶⁰ G. Marchiori,⁶⁰ F. Martinez-Vidal,^{60,†} M. Morganti,⁶⁰ N. Neri,⁶⁰ E. Paoloni,⁶⁰ M. Rama,⁶⁰ G. Rizzo,⁶⁰ F. Sandrelli,⁶⁰ J. Walsh,⁶⁰ M. Haire,⁶¹ D. Judd,⁶¹ K. Paick,⁶¹ D. E. Wagoner,⁶¹ N. Danielson,⁶² P. Elmer,⁶² C. Lu,⁶² V. Miftakov,⁶² J. Olsen,⁶² A. J. S. Smith,⁶² E. W. Varnes,⁶² F. Bellini,⁶³ G. Cavoto,^{62,63} R. Faccini,⁶³ F. Ferrarotto,⁶³ F. Ferroni,⁶³ M. Gaspero,⁶³ L. Li Gioi,⁶³ M. A. Mazzoni,⁶³ S. Morganti,⁶³ M. Pierini,⁶³ G. Piredda,⁶³ F. Safai Tehrani,⁶³ C. Voena,⁶³ S. Christ,⁶⁴ G. Wagner,⁶⁴ R. Waldi,⁶⁴ T. Adye,⁶⁵ N. De Groot,⁶⁵ B. Franek,⁶⁵ N. I. Geddes,⁶⁵ G. P. Gopal,⁶⁵ E. O. Olaiya,⁶⁵ S. M. Xella,⁶⁵ R. Aleksan,⁶⁶ S. Emery,⁶⁶ A. Gaidot,⁶⁶ S. F. Ganzhur,⁶⁶ P.-F. Giraud,⁶⁶ G. Hamel de Monchenault,⁶⁶ W. Kozanecki,⁶⁶ M. Langer,⁶⁶ M. Legendre,⁶⁶ G. W. London,⁶⁶ B. Mayer,⁶⁶ G. Schott,⁶⁶ G. Vasseur,⁶⁶ Ch. Yèche,⁶⁶ M. Zito,⁶⁶ M. V. Purohit,⁶⁷ A. W. Weidemann,⁶⁷ F. X. Yumiceva,⁶⁷ D. Aston,⁶⁸ R. Bartoldus,⁶⁸ N. Berger,⁶⁸ A. M. Boyarski,⁶⁸ O. L. Buchmueller,⁶⁸ M. R. Convery,⁶⁸ M. Cristinziani,⁶⁸ G. De Nardo,⁶⁸ D. Dong,⁶⁸ J. Dorfan,⁶⁸ D. Dujmic,⁶⁸ W. Dunwoodie,⁶⁸ E. E. Elsen,⁶⁸ R. C. Field,⁶⁸ T. Glanzman,⁶⁸ S. J. Gowdy,⁶⁸ T. Hadig,⁶⁸ V. Halyo,⁶⁸ T. Hryn'ova,⁶⁸ W. R. Innes,⁶⁸ M. H. Kelsey,⁶⁸ P. Kim,⁶⁸ M. L. Kocian,⁶⁸ D. W. G. S. Leith,⁶⁸ J. Libby,⁶⁸ S. Luitz,⁶⁸ V. Luth,⁶⁸ H. L. Lynch,⁶⁸ H. Marsiske,⁶⁸ R. Messner,⁶⁸ D. R. Muller,⁶⁸ C. P. O'Grady,⁶⁸ V. E. Ozcan,⁶⁸ A. Perazzo,⁶⁸ M. Perl,⁶⁸ S. Petrak,⁶⁸ B. N. Ratcliff,⁶⁸ A. Roodman,⁶⁸ A. A. Salnikov,⁶⁸ R. H. Schindler,⁶⁸ J. Schwiening,⁶⁸ G. Simi,⁶⁸ A. Snyder,⁶⁸ A. Soha,⁶⁸ J. Stelzer,⁶⁸ D. Su,⁶⁸ M. K. Sullivan,⁶⁸ J. Va'vra,⁶⁸ S. R. Wagner,⁶⁸ M. Weaver,⁶⁸ A. J. R. Weinstein,⁶⁸ W. J. Wisniewski,⁶⁸ M. Wittgen,⁶⁸ D. H. Wright,⁶⁸ C. C. Young,⁶⁸ P. R. Burchat,⁶⁹ A. J. Edwards,⁶⁹ T. I. Meyer,⁶⁹ B. A. Petersen,⁶⁹ C. Roat,⁶⁹ S. Ahmed,⁷⁰ M. S. Alam,⁷⁰ J. A. Ernst,⁷⁰ M. A. Saeed,⁷⁰ M. Saleem,⁷⁰ F. R. Wappler,⁷⁰ W. Bugg,⁷¹ M. Krishnamurthy,⁷¹ S. M. Spanier,⁷¹ R. Eckmann,⁷² H. Kim,⁷² J. L. Ritchie,⁷² A. Satpathy,⁷² R. F. Schwitters,⁷² J. M. Izen,⁷³ I. Kitayama,⁷³ X. C. Lou,⁷³ S. Ye,⁷³ F. Bianchi,⁷⁴ M. Bona,⁷⁴ F. Gallo,⁷⁴ D. Gamba,⁷⁴ C. Borean,⁷⁵ L. Bosisio,⁷⁵ F. Cossutti,⁷⁵ G. Della Ricca,⁷⁵ S. Dittongo,⁷⁵ S. Grancagnolo,⁷⁵ L. Lanceri,⁷⁵ P. Poropat,^{75,‡} L. Vitale,⁷⁵ G. Vuagnin,⁷⁵ R. S. Panvini,⁷⁶ Sw. Banerjee,⁷⁷ C. M. Brown,⁷⁷ D. Fortin,⁷⁷ P. D. Jackson,⁷⁷ R. Kowalewski,⁷⁷ J. M. Roney,⁷⁷ H. R. Band,⁷⁸ S. Dasu,⁷⁸ M. Datta,⁷⁸ A. M. Eichenbaum,⁷⁸ J. J. Hollar,⁷⁸ J. R. Johnson,⁷⁸ P. E. Kutter,⁷⁸ H. Li,⁷⁸ R. Liu,⁷⁸ F. Di Lodovico,⁷⁸ A. Mihalysi,⁷⁸ A. K. Mohapatra,⁷⁸ Y. Pan,⁷⁸ R. Prepost,⁷⁸ S. J. Sekula,⁷⁸ P. Tan,⁷⁸ J. H. von Wimmersperg-Toeller,⁷⁸ J. Wu,⁷⁸ S. L. Wu,⁷⁸ Z. Yu,⁷⁸ and H. Neal⁷⁹

(The BABAR Collaboration)

¹Laboratoire de Physique des Particules, F-74941 Annecy-le-Vieux, France

²Università di Bari, Dipartimento di Fisica and INFN, I-70126 Bari, Italy

³Institute of High Energy Physics, Beijing 100039, China

⁴University of Bergen, Inst. of Physics, N-5007 Bergen, Norway

⁵Lawrence Berkeley National Laboratory and University of California, Berkeley, CA 94720, USA

⁶University of Birmingham, Birmingham, B15 2TT, United Kingdom

⁷Ruhr Universität Bochum, Institut für Experimentalphysik 1, D-44780 Bochum, Germany

⁸University of Bristol, Bristol BS8 1TL, United Kingdom

⁹University of British Columbia, Vancouver, BC, Canada V6T 1Z1

¹⁰Brunel University, Uxbridge, Middlesex UB8 3PH, United Kingdom

¹¹Budker Institute of Nuclear Physics, Novosibirsk 630090, Russia

¹²University of California at Irvine, Irvine, CA 92697, USA

¹³University of California at Los Angeles, Los Angeles, CA 90024, USA

¹⁴University of California at Riverside, Riverside, CA 92521, USA

¹⁵University of California at San Diego, La Jolla, CA 92093, USA

¹⁶University of California at Santa Barbara, Santa Barbara, CA 93106, USA

¹⁷University of California at Santa Cruz, Institute for Particle Physics, Santa Cruz, CA 95064, USA

¹⁸California Institute of Technology, Pasadena, CA 91125, USA

¹⁹University of Cincinnati, Cincinnati, OH 45221, USA

²⁰University of Colorado, Boulder, CO 80309, USA

²¹Colorado State University, Fort Collins, CO 80523, USA

²²Technische Universität Dresden, Institut für Kern- und Teilchenphysik, D-01062 Dresden, Germany

- ²³*Ecole Polytechnique, LLR, F-91128 Palaiseau, France*
- ²⁴*University of Edinburgh, Edinburgh EH9 3JZ, United Kingdom*
- ²⁵*Università di Ferrara, Dipartimento di Fisica and INFN, I-44100 Ferrara, Italy*
- ²⁶*Florida A&M University, Tallahassee, FL 32307, USA*
- ²⁷*Laboratori Nazionali di Frascati dell'INFN, I-00044 Frascati, Italy*
- ²⁸*Università di Genova, Dipartimento di Fisica and INFN, I-16146 Genova, Italy*
- ²⁹*Harvard University, Cambridge, MA 02138, USA*
- ³⁰*Universität Heidelberg, Physikalisches Institut, Philosophenweg 12, D-69120 Heidelberg, Germany*
- ³¹*Imperial College London, London, SW7 2AZ, United Kingdom*
- ³²*University of Iowa, Iowa City, IA 52242, USA*
- ³³*Iowa State University, Ames, IA 50011-3160, USA*
- ³⁴*Laboratoire de l'Accélérateur Linéaire, F-91898 Orsay, France*
- ³⁵*Lawrence Livermore National Laboratory, Livermore, CA 94550, USA*
- ³⁶*University of Liverpool, Liverpool L69 7ZE, United Kingdom*
- ³⁷*Queen Mary, University of London, E1 4NS, United Kingdom*
- ³⁸*University of London, Royal Holloway and Bedford New College, Egham, Surrey TW20 0EX, United Kingdom*
- ³⁹*University of Louisville, Louisville, KY 40292, USA*
- ⁴⁰*University of Manchester, Manchester M13 9PL, United Kingdom*
- ⁴¹*University of Maryland, College Park, MD 20742, USA*
- ⁴²*University of Massachusetts, Amherst, MA 01003, USA*
- ⁴³*Massachusetts Institute of Technology, Laboratory for Nuclear Science, Cambridge, MA 02139, USA*
- ⁴⁴*McGill University, Montréal, QC, Canada H3A 2T8*
- ⁴⁵*Università di Milano, Dipartimento di Fisica and INFN, I-20133 Milano, Italy*
- ⁴⁶*University of Mississippi, University, MS 38677, USA*
- ⁴⁷*Université de Montréal, Laboratoire René J. A. Lévesque, Montréal, QC, Canada H3C 3J7*
- ⁴⁸*Mount Holyoke College, South Hadley, MA 01075, USA*
- ⁴⁹*Università di Napoli Federico II, Dipartimento di Scienze Fisiche and INFN, I-80126, Napoli, Italy*
- ⁵⁰*NIKHEF, National Institute for Nuclear Physics and High Energy Physics, NL-1009 DB Amsterdam, The Netherlands*
- ⁵¹*University of Notre Dame, Notre Dame, IN 46556, USA*
- ⁵²*Oak Ridge National Laboratory, Oak Ridge, TN 37831, USA*
- ⁵³*Ohio State University, Columbus, OH 43210, USA*
- ⁵⁴*University of Oregon, Eugene, OR 97403, USA*
- ⁵⁵*Università di Padova, Dipartimento di Fisica and INFN, I-35131 Padova, Italy*
- ⁵⁶*Universités Paris VI et VII, Lab de Physique Nucléaire H. E., F-75252 Paris, France*
- ⁵⁷*Università di Pavia, Dipartimento di Elettronica and INFN, I-27100 Pavia, Italy*
- ⁵⁸*University of Pennsylvania, Philadelphia, PA 19104, USA*
- ⁵⁹*Università di Perugia, Dipartimento di Fisica and INFN, I-06100 Perugia, Italy*
- ⁶⁰*Università di Pisa, Dipartimento di Fisica, Scuola Normale Superiore and INFN, I-56127 Pisa, Italy*
- ⁶¹*Prairie View A&M University, Prairie View, TX 77446, USA*
- ⁶²*Princeton University, Princeton, NJ 08544, USA*
- ⁶³*Università di Roma La Sapienza, Dipartimento di Fisica and INFN, I-00185 Roma, Italy*
- ⁶⁴*Universität Rostock, D-18051 Rostock, Germany*
- ⁶⁵*Rutherford Appleton Laboratory, Chilton, Didcot, Oxon, OX11 0QX, United Kingdom*
- ⁶⁶*DSM/Dapnia, CEA/Saclay, F-91191 Gif-sur-Yvette, France*
- ⁶⁷*University of South Carolina, Columbia, SC 29208, USA*
- ⁶⁸*Stanford Linear Accelerator Center, Stanford, CA 94309, USA*
- ⁶⁹*Stanford University, Stanford, CA 94305-4060, USA*
- ⁷⁰*State Univ. of New York, Albany, NY 12222, USA*
- ⁷¹*University of Tennessee, Knoxville, TN 37996, USA*
- ⁷²*University of Texas at Austin, Austin, TX 78712, USA*
- ⁷³*University of Texas at Dallas, Richardson, TX 75083, USA*
- ⁷⁴*Università di Torino, Dipartimento di Fisica Sperimentale and INFN, I-10125 Torino, Italy*
- ⁷⁵*Università di Trieste, Dipartimento di Fisica and INFN, I-34127 Trieste, Italy*
- ⁷⁶*Vanderbilt University, Nashville, TN 37235, USA*
- ⁷⁷*University of Victoria, Victoria, BC, Canada V8W 3P6*
- ⁷⁸*University of Wisconsin, Madison, WI 53706, USA*
- ⁷⁹*Yale University, New Haven, CT 06511, USA*

(Dated: October 10, 2018)

We report a measurement of the production ratio of charged and neutral B mesons from $\Upsilon(4S)$ decays based on the ratio of efficiency-corrected yields for the charmonium modes $J/\psi K^+$ and $J/\psi K_S^0$ with 81.9 fb^{-1} of data collected with the BABAR detector on the $\Upsilon(4S)$ resonance at 10.580 GeV . We find a value of $1.006 \pm 0.036(\text{stat}) \pm 0.031(\text{sys})$ for the ratio $R^{+/0} = \Gamma(\Upsilon(4S) \rightarrow B^+ B^-) / \Gamma(\Upsilon(4S) \rightarrow B^0 \bar{B}^0)$.

A measurement of the B^+/B^0 production ratio

$$R^{+/0} = \frac{\Gamma(\Upsilon(4S) \rightarrow B^+B^-)}{\Gamma(\Upsilon(4S) \rightarrow B^0\bar{B}^0)}$$

from the $\Upsilon(4S)$ meson is an essential element in determining branching fractions and quark-mixing matrix elements at the B factory experiments. It can also provide information about the structure of the $\Upsilon(4S)$ meson that can be used to discriminate between available models.

Over the past 15 years it has been frequently assumed that $R^{+/0}$ is equal to one, although many models predict that this may not be the case. Early calculations predicted that the ratio could be up to 20% greater than one, due to large Coulomb corrections [1]. Taking into account the structure of the B and $\Upsilon(4S)$ reduces the effect of the Coulomb interaction and can even lead to the ratio being less than unity [2]. With the prospect of precision measurements from the B factories, there has been a recent revival in theoretical work on the subject. A more detailed calculation has been done in a non-relativistic effective field theory with B^* intermediate states in the pion potential, which introduces isospin-breaking in strong interactions. These calculations predict a value 1.1–1.2 [3]. Other calculations attempting to take into account the structure of the mesons and hadronic final state interactions predict a ratio 0.9–1.2 [4], but with rapid variation as a function of the center-of-mass energy near the $\Upsilon(4S)$ resonance. However, such rapid variation in the charged-to-neutral ratio has not been seen in scans across the $\phi(1020)$ resonance [5]. For the $\Upsilon(4S)$, there are published measurements of $R^{+/0}$ by CLEO ($1.04 \pm 0.07 \pm 0.04$ [6], $1.058 \pm 0.084 \pm 0.136$ [7]), BABAR ($1.10 \pm 0.06 \pm 0.05$ [8] with 20 fb^{-1}), and Belle ($1.01 \pm 0.03 \pm 0.09$ [9] with 29 fb^{-1}). Now that a significantly larger $\Upsilon(4S)$ data sample is available at BABAR we can reduce the statistical uncertainty to the point where it is possible to confront the various theoretical predictions.

In this analysis we use the decay modes $B^0 \rightarrow J/\psi K_s^0$ and $B^+ \rightarrow J/\psi K^+$ [10], where $J/\psi \rightarrow \ell^+\ell^-$ and $K_s^0 \rightarrow \pi^+\pi^-$, to measure the B^+/B^0 production ratio. These decays are good candidates for measuring $R^{+/0}$ since isospin violation in the $B \rightarrow J/\psi K$ decays is expected to be small in the Standard Model, of order $\lambda^3 \approx 0.01$ [11] when rescattering is small, where λ is defined as the sine of the Cabibbo angle.

The data used in this analysis were collected with the BABAR detector at the PEP-II e^+e^- storage ring. The data sample corresponds to 81.9 fb^{-1} of integrated luminosity collected at the $\Upsilon(4S)$ resonance. The distribution of center-of-mass energies due to the beam-energy spread is Gaussian with $\sigma = 4.6 \text{ MeV}$ [12]. The mean energy of our sample is 10.580 GeV , with all data accumulated within one sigma of this value.

The BABAR detector is fully described elsewhere [13]. It consists of a charged-particle tracking system, a Cherenkov detector (DIRC) for particle identification, an electromagnetic calorimeter, and a system for muon identification. The tracking system consists of a 5-layer, double-sided silicon vertex tracker and a 40-layer drift chamber (filled with a mixture of helium and isobutane), both in a 1.5-T magnetic field supplied by a superconducting solenoidal magnet. The DIRC is an imaging Cherenkov detector relying on total internal reflection in the radiator. The electromagnetic calorimeter consists of 6580 CsI(Tl) crystals. The iron flux return is segmented and instrumented with resistive plate chambers for muon identification.

Hadronic events are selected by requiring the presence of at least three tracks in the angular region $0.41 < \theta_{\text{LAB}} < 2.54 \text{ rad}$, where θ_{LAB} is the polar angle with respect to the beam direction. The ratio between the 2nd and 0th order Fox-Wolfram [14] moments must be less than 0.5. We also require that the total energy of all particles in the event be greater than 4.5 GeV . The primary vertex, which is constructed from charged tracks with impact parameter less than 1mm in the plane transverse to the beam direction, must be within 0.5 cm of the beam spot in the plane transverse to the beam direction and within 6 cm along the beam direction.

We reconstruct candidates for J/ψ mesons in the decay modes $J/\psi \rightarrow e^+e^-$ and $\mu^+\mu^-$. For $J/\psi \rightarrow e^+e^-$ decays one track is required to pass a tight electron selection and the other a loose requirement [8], while for $J/\psi \rightarrow \mu^+\mu^-$ decays we require one track to pass a loose muon selection and the other a minimum-ionizing requirement [8]. The daughter tracks of the J/ψ candidate are required to have 12 hits in the drift chamber, lie in the angular range $0.41 < \theta_{\text{LAB}} < 2.409 \text{ rad}$ for electrons and $0.41 < \theta_{\text{LAB}} < 2.54 \text{ rad}$ for muons, and have a transverse momentum of at least $100 \text{ MeV}/c$. To increase the efficiency of the event selection, electron candidate tracks are combined with photon candidates to recover some of the energy lost in bremsstrahlung [8]. A geometric vertex constraint fit is applied to the lepton track pair. The invariant mass requirements for the $J/\psi \rightarrow e^+e^-$ and $J/\psi \rightarrow \mu^+\mu^-$ channels are $2.95 < M_{e^+e^-} < 3.14 \text{ GeV}/c^2$ and $3.06 < M_{\mu^+\mu^-} < 3.14 \text{ GeV}/c^2$. We require $|\cos\theta_\ell|$ to be less than 0.8 and 0.9 for $J/\psi \rightarrow e^+e^-$ and $J/\psi \rightarrow \mu^+\mu^-$ respectively. The helicity angle θ_ℓ is the angle in the J/ψ rest frame between the positively charged J/ψ daughter and the reversed K flight direction in the B meson rest frame.

We reconstruct K_s^0 meson candidates from two charged tracks, which are not required to originate from the interaction point or to have drift chamber hits, in contrast to the J/ψ daughters. The tracks are assigned the pion

mass to compute $M_{\pi^+\pi^-}$, which is required to lie in the range $0.490 - 0.505 \text{ GeV}/c^2$. Also, in order to reject combinatorial background, we only retain candidates with a fitted K_s^0 vertex displaced more than 1 mm from the J/ψ vertex. Candidates for K^+ mesons are assigned the kaon mass and are required to form a vertex with the J/ψ candidate. No particle identification requirements are made for this track.

The selection of B candidates relies on the kinematic constraints given by the $\Upsilon(4S)$ initial state. Two largely uncorrelated variables are used: the energy-substituted B mass $m_{\text{ES}} = \sqrt{(s/2 + \mathbf{p}_0 \cdot \mathbf{p}_B)^2/E_0^2 - p_B^2}$, where the subscripts 0 and B refer to the e^+e^- system and the B candidate respectively, s is the square of the center-of-mass energy, and energies (E) and momentum vectors (\mathbf{p}) are computed in the laboratory frame; and $\Delta E = E_B^* - \sqrt{s}/2$, where E_B^* is the B candidate energy in the center-of-mass frame. In cases where multiple B candidates are present in the same event, 2% of the total, only the one with the smallest absolute value of ΔE is retained.

The signal region in the $m_{\text{ES}}-\Delta E$ plane is defined by $5.27 < m_{\text{ES}} < 5.29 \text{ GeV}/c^2$ and $|\Delta E| < 3\sigma(\Delta E)$. The observed resolutions for data and Monte Carlo for the different modes are listed in Table I. The m_{ES} sideband is defined by $5.20 < m_{\text{ES}} < 5.27 \text{ GeV}/c^2$ and $|\Delta E| < 3\sigma(\Delta E)$. Upper and lower ΔE sidebands, used for the evaluation of systematic errors, are defined as $50 < \Delta E < 120 \text{ MeV}$ and $-120 < \Delta E < -50 \text{ MeV}$.

Since we are measuring the ratio of B^+ to B^0 efficiency-corrected yields many of the selection requirements are in common and have been optimized previously [8]. Therefore for this analysis, we have only reconsidered the optimization of the statistical uncertainty of the measurement due to those requirements that are different for the two modes. These requirements include the K_s^0 flight length, K_s^0 mass window, and the ΔE window. The optimization of these variables maximizes the ratio $N_{\text{cand}}/\sqrt{\sigma^2(N_{\text{cand}}) + \sigma^2(N_{\text{bkg}})}$ where $\sigma(N_{\text{cand}})$ and $\sigma(N_{\text{bkg}})$ are the uncertainties on the number of signal candidates N_{cand} predicted by Monte Carlo (MC) simulation and combinatorial background N_{bkg} , respectively, that pass the event selection procedure. N_{cand} is defined as number of events in the signal region.

TABLE I: Summary of the resolution for ΔE in data and MC simulation.

Mode	$\sigma(\Delta E)$ [MeV]	
	MC	Data
B^- J/ψ		
B^+ e^+e^-	11.42 ± 0.11	10.87 ± 0.25
B^+ $\mu^+\mu^-$	9.72 ± 0.07	9.25 ± 0.20
B^0 e^+e^-	9.50 ± 0.11	10.02 ± 0.42
B^0 $\mu^+\mu^-$	7.92 ± 0.07	8.52 ± 0.32

We fit the m_{ES} distribution in the m_{ES} sideband with

an empirical phase-space-motivated function introduced by ARGUS [15]. The fitted distribution is then integrated over the signal region to determine the number of combinatorial background events N_{bkg} . In addition to combinatorial backgrounds there are other background sources, mostly in B decays to charmonium, that peak near the B mass in m_{ES} . These peaking sources are negligible for the neutral B sample, but include small contributions from $B^0 \rightarrow J/\psi K_s^0$ and $B^+ \rightarrow J/\psi \pi^+$ for the charged B sample. Requiring particle identifications on the K^+ candidate will reduce these contributions but introduces a larger systematic error. To determine the number of background events that peak in the m_{ES} signal region, N_{peak} , we use appropriately combined MC samples of continuum e^+e^- and generic [16] $B\bar{B}$ events (with signal events removed), which have been scaled to the integrated luminosity of the data sample. This distribution is then fitted with an ARGUS function as described above. We determine N_{peak} by counting the number of events in the signal region and subtracting the integral of the ARGUS function over this same region. The signal yield is then defined by $N_{\text{signal}} = N_{\text{cand}} - N_{\text{bkg}} - N_{\text{peak}}$. The observed distributions in m_{ES} and ΔE for $B^0 \rightarrow J/\psi K_s^0$ and $B^+ \rightarrow J/\psi K^+$ candidates in data are shown in Figs. 1 and 2 respectively.

The efficiency-corrected ratio of observed events is given by:

$$\begin{aligned} \frac{N_{\text{signal}}^+/\epsilon_+}{N_{\text{signal}}^0/(f\epsilon_0)} &= R^{+/0} \frac{\mathcal{B}(B^+ \rightarrow J/\psi K^+)}{\mathcal{B}(B^0 \rightarrow J/\psi K_s^0)} \\ &= R^{+/0} \frac{2\Gamma(B^+ \rightarrow J/\psi K^+)\tau_+}{\Gamma(B^0 \rightarrow J/\psi K^0)\tau_0} \end{aligned}$$

where $f = 68.60 \pm 0.27\%$ [17] is the $K_s^0 \rightarrow \pi^+\pi^-$ branching fraction, $\tau_+/\tau_0 = 1.083 \pm 0.017$ [17] is the ratio of B^+ and B^0 lifetimes, and ϵ is the selection efficiency. Therefore, assuming isospin invariance in the $B \rightarrow J/\psi K$ decay, $\Gamma(B^+ \rightarrow J/\psi K^+) = \Gamma(B^0 \rightarrow J/\psi K^0)$ [18], the ratio of efficiency-corrected yields is determined from:

$$R^{+/0} = \frac{N_{\text{signal}}^+ \epsilon_0 f \tau_0}{2N_{\text{signal}}^0 \epsilon_+ \tau_+}. \quad (1)$$

The ratio of efficiency-corrected yields is determined separately for $J/\psi \rightarrow e^+e^-$ and $J/\psi \rightarrow \mu^+\mu^-$ so that lepton identification efficiencies cancel. The separate measurements are then averaged, keeping track of correlated uncertainties, to produce a final value for $R^{+/0}$.

Sources of systematic uncertainties can be classified into those arising from uncertainties on efficiencies and those from candidate selection and backgrounds. The efficiency uncertainties are due to K_s^0 reconstruction, tracking, and kaon/pion tracking efficiency differences. In the ratio of the efficiency-corrected yields, the tracking uncertainty is due to the extra track required to reconstruct the $B^0 \rightarrow J/\psi K_s^0$ mode. We determine the

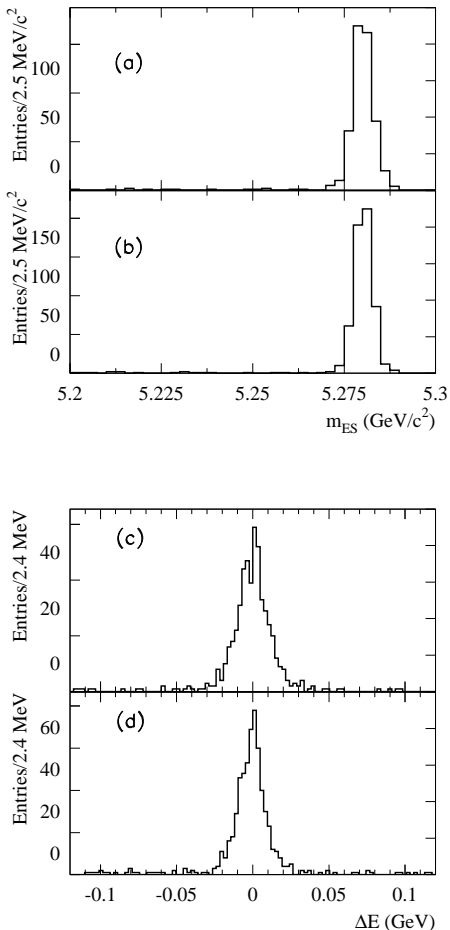


FIG. 1: Distribution of m_{ES} for $|\Delta E| < 3\sigma$ in the $B^0 \rightarrow J/\psi K_s^0$ sample for (a) $J/\psi \rightarrow e^+e^-$ and (b) $J/\psi \rightarrow \mu^+\mu^-$. Distribution of ΔE for $m_{ES} > 5.27 \text{ GeV}/c^2$ in the $B^0 \rightarrow J/\psi K_s^0$ sample for (c) $J/\psi \rightarrow e^+e^-$ and (d) $J/\psi \rightarrow \mu^+\mu^-$.

relative kaon/pion tracking reconstruction efficiency by comparing the ratio of efficiencies for $B^+ \rightarrow J/\psi K^+$ and $B^+ \rightarrow J/\psi \pi^+$ Monte Carlo. The systematic error of 0.6% is taken to be half the size of the estimated difference. Finally, for the uncertainty on the K_s^0 efficiency we take a sample of inclusive K_s^0 candidates that are binned in transverse momentum (p_T), laboratory polar angle (θ_{LAB}), and transverse flight length (dr). A relative correction for reconstruction of a displaced K_s^0 candidate is determined in each p_T and θ_{LAB} bin by assuming the tracking efficiency for a short-lived K_s^0 close to the interaction region is the same as for prompt tracks. Thus, the ratio of data to MC relative efficiency is normalized to unity for small dr and then used to derive a MC correction factor for larger displacements. By varying the size of the dr , p_T , and θ_{LAB} bins we determine a systematic uncertainty for this procedure. The normalization bin for the correction is well inside the radius of the beam

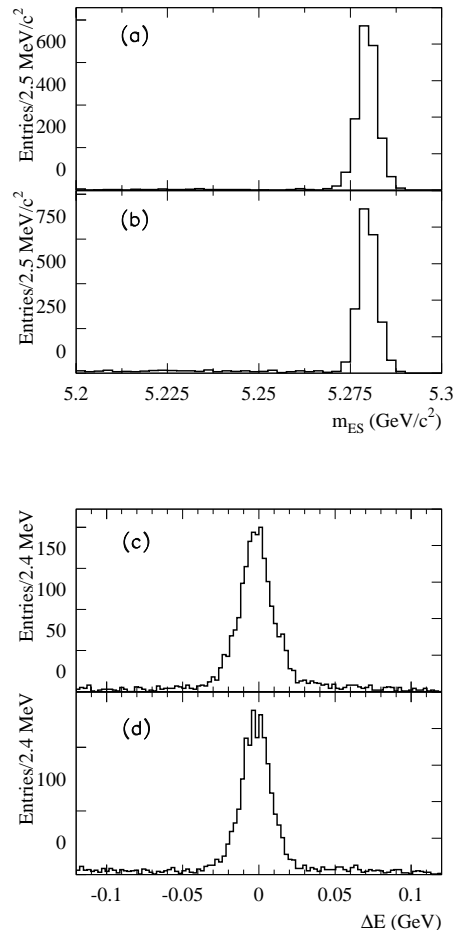


FIG. 2: Distribution of m_{ES} for $|\Delta E| < 3\sigma$ in the $B^+ \rightarrow J/\psi K^+$ sample for (a) $J/\psi \rightarrow e^+e^-$ and (b) $J/\psi \rightarrow \mu^+\mu^-$. Distribution of ΔE for $m_{ES} > 5.27 \text{ GeV}/c^2$ in the $B^+ \rightarrow J/\psi K^+$ for (c) $J/\psi \rightarrow e^+e^-$ and (d) $J/\psi \rightarrow \mu^+\mu^-$.

pipe. We vary the definition of this bin as a check of the hypothesis that these tracks have the same efficiency as normal charged tracks.

TABLE II: Summary of the relative systematic uncertainties on the efficiency-corrected yields.

Mode	Parameters (%)							
	J/ψ	ϵ_{Trk}	ϵ_{K^+/π^+}	$\epsilon_{K_s^0}$	ARGUS Bkgd.	Peaking Bkgd.	Vary Selection	Total
$B^+ e^+e^-$	-	0.6	-	0.5	0.1	0.1	0.1	0.8
$B^+ \mu^+\mu^-$	-	0.6	-	0.6	0.4	1.0	1.0	1.4
$B^0 e^+e^-$	1.3	-	1.8	0.8	0.1	0.2	0.2	2.4
$B^0 \mu^+\mu^-$	1.3	-	1.8	0.5	0.1	1.3	2.6	

The selection and background systematic uncertainties are attributed to the selection criteria, the ARGUS background shape, and the peaking background subtraction.

The selection requirements on the K_s^0 mass, K_s^0 flight distance, and ΔE are varied within reasonable ranges. The K_s^0 mass and ΔE selection windows were increased and decreased from the nominal value by half a sigma and the K_s^0 vertex displacement requirement was removed. The largest difference from the nominal efficiency-corrected yield is taken conservatively as a systematic uncertainty. The continuum background systematic uncertainty is determined by varying the ARGUS parameter by two sigma to account for any model dependence. The peaking background uncertainty is evaluated from the discrepancy between data and MC in the the upper and lower ΔE sidebands. The larger of the two discrepancies is taken as the systematic uncertainty. This is a more conservative approach than using the uncertainties for the relevant branching fractions. Table II summarizes the sources of systematic uncertainty for this analysis.

TABLE III: Summary of values needed to determine the efficiency corrected yields.

Mode	Parameters				
	J/ψ	N_{cand}	N_{bkg}	N_{peak}	Efficiency (%)
B^+	e^+e^-	2213	19.5 ± 5.0	9.6 ± 3.2	40.8 ± 0.4
B^0	e^+e^-	502	2.6 ± 2.0	2.4 ± 1.5	29.9 ± 0.4
B^+	$\mu^+\mu^-$	2497	50.6 ± 7.2	33.5 ± 4.6	47.8 ± 0.4
B^0	$\mu^+\mu^-$	577	2.0 ± 1.5	2.4 ± 2.1	35.6 ± 0.4

Table III lists the efficiencies, background composition, and number of events in the signal region based on the one-dimensional fit with a $3(\sigma)$ ΔE requirement. Based on Eq.(1) we determine:

$$\begin{aligned}
 R^{+/0}(e^+e^-) &= 1.019 \pm 0.054(\text{stat}) \pm 0.031(\text{sys}) \\
 R^{+/0}(\mu^+\mu^-) &= 0.994 \pm 0.049(\text{stat}) \pm 0.033(\text{sys}) \\
 R^{+/0}(\text{avg}) &= 1.006 \pm 0.036(\text{stat}) \pm 0.031(\text{sys})
 \end{aligned}$$

when assuming isospin conservation in $B \rightarrow J/\psi K$ decays. The data sample has a mean energy of 10.580 GeV and does not have sufficient spread to test the hypothesis of an energy dependent production ratio.

We have confirmed that the result for the individual efficiency-corrected signal yields for the $J/\psi \rightarrow e^+e^-$ and $J/\psi \rightarrow \mu^+\mu^-$ channels is consistent among seven equal subsets of the full sample, as is the ratio of $e^+e^-/\mu^+\mu^-$.

To check our fitting technique we have performed a two-dimensional non-parametric fit to the data. This is done by fitting the data to a sum of contributions from five different sources ($e^+e^- \rightarrow q\bar{q}$, $e^+e^- \rightarrow c\bar{c}$, generic $\Upsilon(4S) \rightarrow B^0\bar{B}^0$, generic $\Upsilon(4S) \rightarrow B^+B^-$, and signal) whose densities [19] in ΔE and m_{ES} are determined from a non-parametric fit to candidates from Monte Carlo samples. The two-dimensional fit is done in the region $5.200 < m_{\text{ES}} < 5.270 \text{ GeV}/c^2$ and $0.030 < |\Delta E| < 0.120 \text{ GeV}$. This technique has the advantage that we

are not restricted to a small range in $|\Delta E|$. It also employs the MC predicted background distributions, rather than the empirical shape imposed by the ARGUS function. The non-parametric fit method finds results that are consistent with the simpler counting method, both for the full sample and for data subsets.

The observed value for $R^{+/0}$ is close to one, as has been assumed by most branching fraction measurements obtained on the $\Upsilon(4S)$, with a ratio as large as 1.2 disfavored at the four sigma level. Our measurement will aid in restricting models of $\Upsilon(4S)$ decays. It also allows a quantitative determination of the contribution from $R^{+/0}$ to all branching fractions that are determined at the B factories operating on the $\Upsilon(4S)$ resonance. We are grateful for the excellent luminosity and machine conditions provided by our PEP-II colleagues, and for the substantial dedicated effort from the computing organizations that support *BABAR*. The collaborating institutions wish to thank SLAC for its support and kind hospitality. This work is supported by DOE and NSF (USA), NSERC (Canada), IHEP (China), CEA and CNRS-IN2P3 (France), BMBF and DFG (Germany), INFN (Italy), FOM (The Netherlands), NFR (Norway), MIST (Russia), and PPARC (United Kingdom). Individuals have received support from the A. P. Sloan Foundation, Research Corporation, and Alexander von Humboldt Foundation.

* Also with Università della Basilicata, Potenza, Italy

† Also with IFIC, Instituto de Física Corpuscular, CSIC-Universidad de Valencia, Valencia, Spain

‡ Deceased

- [1] D.Atwood and W.J.Marciano, Phys. Rev. D **41**, 1736 (1990).
- [2] G.P.Lepage, Phys. Rev. D **42**, 3251 (1990).
- [3] R.Kaiser, A.V.Manohar, and T.Mehen, Phys. Rev. Lett. **90**, 142001 (2003).
- [4] M.B.Voloshin, Mod. Phys. Lett. **A18**, 1783 (2003).
- [5] SND Collaboration, M.N. Achasov *et al.*, Phys. Rev. D **63**, 072002 (2001).
- [6] CLEO Collaboration, J.P.Alexander *et al.*, Phys. Rev. Lett. **86**, 2737 (2001).
- [7] CLEO Collaboration, S.B.Athar *et al.*, Phys. Rev. D **66**, 052003 (2002).
- [8] *BABAR* Collaboration, B.Aubert *et al.*, Phys. Rev. D **65**, 032001 (2002).
- [9] Belle Collaboration, N.C.Hastings *et al.*, Phys. Rev. D **67**, 052004 (2003).
- [10] Charge conjugate decays are implied throughout this paper. Results are averages over both charge conjugate states.
- [11] R. Fleischer, and T. Mannel, Phys. Lett. B **506**, 311-322 (2001).
- [12] *BABAR* Collaboration, B.Aubert *et al.*, hep-ex/0308020, August 2003.
- [13] *BABAR* Collaboration, B.Aubert *et al.*, Nucl. Instr. Meth. A **479**, 1 (2002).

- [14] G.C. Fox and S. Wolfram, Nucl. Phys. B **149**, 413 (1979).
- [15] ARGUS Collaboration, H. Albrecht *et al.*, Z. Phys. C **48**, 543 (1990).
- [16] Generic B events include known B decays with measured branching fractions and hadronized quark model decays for unknown branching fractions.
- [17] Particle Data Group, K. Hagiwara *et al.*, Phys. Rev. D **66**, 010001 (2002).
- [18] The phase space difference between these two decays is negligible.
- [19] “Density Estimation”, B. W. Silverman, CRC Press, ISBN: 0412246201 (1986).